UDK 666.3/.7:621.762.5
Original scientific article/Izvirni znanstveni članek

ISSN 1580-2949
MTAEC9, 49(6)975(2015)

SOLID-STATE SINTERING OF $(K_{0.5}Na_{0.5})NbO_3$ SYNTHESIZED FROM AN ALKALI-CARBONATE-BASED LOW-TEMPERATURE CALCINED POWDER

SINTRANJE V TRDNEM KERAMIKE $(K_{0,5}Na_{0,5})NbO_3$, SINTETIZIRANE IZ NIZKOTEMPERATURNO KALCINIRANEGA PRAHU, PRIPRAVLJENEGA NA OSNOVI ALKALIJSKIH KARBONATOV

Mahdi Feizpour[1], Touradj Ebadzadeh[1], Darja Jenko[2]

[1]Department of Ceramic Engineering, Materials and Energy Research Center, P.O. Box 31787-316, Karaj, Alborz, Iran
[2]Institute of Metals and Technology, Lepi pot 11, 1000 Ljubljana, Slovenia
m-feizpour@merc.ac.ir, iusteng@gmail.com

Prejem rokopisa – received: 2015-10-10; sprejem za objavo – accepted for publication: 2015-10-19

doi:10.17222/mit.2015.315

Potassium sodium niobate $K_{0.5}Na_{0.5}NbO_3$ (KNN) was synthesized by the double calcination of a homogenized mixture of potassium and sodium carbonates and niobium pentoxide for 4 h at 625 °C. The calcination temperature was chosen on the basis of the thermal analyses of the mixture of precursors, where the weight loss being the function of the temperature reaches the plateau. The calcined powder was investigated by X-ray Diffraction (XRD) and Transmission Electron Microscopy (TEM) and was found to be without unreacted materials or secondary phases. Before sintering, the powder compacts were annealed for 4 h at 450 °C, while the sintering was carried out for 2 h at 1115 °C using two different configurations: 1) in a closed crucible where the KNN pellets were in close physical proximity to, but not in direct contact with, the KNN packing powder, and 2) in a completely open crucible without any packing powder. The Archimedes' density of the sintered samples was 91.5 % of theoretical density for the first configuration, while it was 93.4 % for the second configuration. The Field-Emission Scanning Electron Microscopy (FE-SEM) and XRD analyses of the sintered ceramics showed that by using a calcination temperature as low as 625 °C a typical sintered microstructure of KNN could be achieved with both sintering configurations.

Keywords: potassium sodium niobate, low-temperature calcination, solid-state synthesis, sintering, microstructure

Keramiko kalij-natrijevega niobata $K_{0,5}Na_{0,5}NbO_3$ (KNN) smo sintetizirali z dvojno kalcinacijo homogenizirane zmesi kalijevega in natrijevega karbonata ter niobijevega oksida 4 h pri temperaturi 625 °C. Temperaturo kalicinacije smo izbrali glede na termično analizo mešanice prekurzorjev, kjer se izguba mase v odvisnosti od temperature ni več spreminjala in je dosegla plato. Kalciniran prah smo preiskovali z rentgensko fazno analizo (XRD) in presevno elektronsko mikroskopijo (TEM), ki sta pokazali, da prah ne vsebuje nezreagiranih materialov ali sekundarnih faz. Stisnjene tabletke kaciniranega prahu so bile pred sintranjem segrevane 4 h pri 450 °C, samo sintranje pa je potekalo 2 h pri 1115 °C z uporabo dveh različnih konfiguracij: 1) v zaprtem lončku, kjer so bile tabletke KNN v neposredni fizični bližini, a ne v neposrednem stiku z zasipom KNN in 2) v popolnoma odprtem lončku brez zasipa. Povprečna Arhimedova gostota sintranih vzorcev je bila za prvo konfiguracijo 91,5 % teoretične gostote, medtem ko je bila za drugo konfiguracijo 93,4 %. Vrstična elektronska mikroskopija z emisijo polja (FE-SEM) in analiza XRD sintrane keramike sta pokazali, da lahko že pri nižji temperaturi kalciniranja 625 °C dosežemo tipično sintrano mikrostrukturo KNN za obe konfiguraciji sintranja.

Ključne besede: kalij-natrijev niobat, nizkotemperaturna kalcinacija, sinteza v trdnem stanju, sintranje, mikrostruktura

1 INTRODUCTION

Pb-based piezoceramics are the main group of piezoelectric materials with high electromechanical properties.[1] However, with the beginning of the 21st Century, some legislation was imposed to limit the fabrication and usage of substances that contain lead, due to its toxicity, and to develop environmentally friendlier replaceable materials.[2] During the past 15 years, different families of known lead-free piezoelectrics were restudied and several attempts were focused on obtaining functional properties close to those of the lead-based piezoelectrics.[3–5]

Among the different groups of lead-free piezoelectric ceramics, the potassium sodium niobate $K_{0.5}Na_{0.5}NbO_3$ [KNN] family is a widely investigated candidate for the replacement of $Pb(Zr,Ti)O_3$ and the other lead-based piezoelectric ceramics, mainly due to its fair electromechanical properties, high Curie point and its compatibility with base-metal electrodes like Ni.[6–14] Dealing with KNN-based materials involves some difficulties, mainly concerning the preservation of the stoichiometry during the powder synthesis and the sintering of the powder compact, because of the high potential of the alkali elements for evaporation, especially at elevated temperatures.[15,16]

Up to now, numerous studies have been conducted on maximizing the piezoelectric response of pure and/or doped KNN-based lead-free piezoelectric ceramics. However, since the major and cheapest source for providing alkali elements for the synthesis of KNN is alkali carbonates of Na_2CO_3 and K_2CO_3, the calcination of the homogenized KNN precursors is an important step

in the solid-state synthesis of KNN. The most widely used temperatures for the calcination of KNN from the alkali carbonates are in the range between 750 °C and 950 °C.[9] But as Popovic et al.[16] have thermodynamically shown, the vapor pressure of alkali elements over the respective niobates increases by 4 to 5 orders of magnitudes when increasing the temperature from 627 °C to 927 °C. This makes the low-temperature calcination process an easy solution to overcome the off-stoichiometry problem for the synthesized KNN powder due to the evaporation of the alkali elements at elevated temperatures. On the other hand, using lower calcination temperatures may lead to powders with a lower crystallinity and still-unreacted precursors. Based on the literature and the best of our knowledge, up to now, the lowest temperature of synthesis for KNN powder from a Na_2CO_3, K_2CO_3 and Nb_2O_5 mixture was 700 °C.[17] The aim of this study is to explore whether this temperature can be even more reduced and the sintered properties of samples still remain good enough or not.

2 MATERIALS AND METHODS

Na_2CO_3 (99.95–100.05 % purity), K_2CO_3 (99+ % purity) and Nb_2O_5 (99.9 % purity), all from Sigma-Aldrich, Germany, were dried over night at 200 °C and weighed according to the $K_{0.5}Na_{0.5}NbO_3$ stoichiometry in a dry-box and homogenized in a PM-400 Retsch planetary mill for 4 h at 175 r/min using 125 mL grinding zirconia jar and zirconia balls (3 mm in diameter) and 99.8 % purity acetone as the medium. The homogenized mixture of KNN precursors (hereafter, HOM powder) was dried for 1 h at 90 °C and at least 2 h at 200 °C and stored in a desiccator.

Differential Thermal Analysis (DTA) and Thermo-Gravimetry (TG) of the HOM powder were recorded from 200 °C to 750 °C with a heating rate of 10 °C/min by means of a Netzsch STA 409 C/CD under a constant flow rate of 100 cm^3/min of dried synthetic air. Prior to the measurement, the sample was isothermally held for 3 h at 200 °C. In addition, the dimensional changes vs. the temperature of the HOM and calcined powder compact (100 MPa, uniaxial press) were recorded from 200 °C to 1200 °C with a heating rate of 5 °C/min under synthetic air using a Leitz optical dilatometry. The X-ray Diffraction (XRD) patterns of the calcined powders and the crushed sintered pellets were recorded at room temperature using a PANalytical X'Pert PRO MPD diffractometer with Cu-$K\alpha_1$ radiation of 0.15406 nm in the 2θ range 10–90 ° with a step of 0.017 ° and an integration time of 200 s.

The particle size distribution of the calcined powder was analyzed with a Microtrac S3500 static light-scattering particle size analyzer. The specific surface area of the calcined powder was analyzed by nitrogen adsorption/desorption at –196 °C (BET method, Belsorp-mini II) using an automated gas-adsorption analyzer. Prior to the measurement, the powders were degassed under vacuum for 2 h at 250 °C. The morphology, crystal structure and elemental composition of the calcined powder were observed and analyzed with a High-Resolution Transmission Electron Microscope (HR-TEM – JEOL JEM-2100) using an accelerating voltage 200 kV with an attached Energy-Dispersive X-ray Spectrometer EDS (JEOL JED-2300 Series) and a Scanning Transmission Electron Microscope (STEM) unit with a Bright-Field (BF) detector (EM-24511SIOD, JEOL).

After the calcination process, the powders were compacted at 200 MPa using a cold isostatic press. Before sintering, the powder compacts were annealed for 4 h at 450 °C in order to remove the adsorbed moisture and CO_2 from the powder before the sintering process started. The sintering was carried out for 2 h at 1115 °C using two different configurations: 1) in a closed, double-crucible (high-purity alumina, total volume: ≈ 16 cm^3) where the KNN pellets were put in a small Pt crucible (volume: ≈ 2 cm^3), which was surrounded by KNN packing powder (2.5 g, after the first calcination at 800 °C), hereafter the CC/wPP configuration, and 2) in a completely open crucible where the KNN pellets were put in a small Pt crucible without using any packing powder, hereafter the OC/woPP configuration. The density of the sintered ceramics was measured based on Archimedes' principle using the ASTM C373 standard and reported as an average value of three measurements. The sintered pellets were cut, mounted, and polished using standard ceramography techniques and finished with 3 μm and ¼ μm diamond-paste polishes. The microstructure of the sintered ceramics was characterized using a Field-Emission Scanning Electron Microscope (FE-SEM – JEOL JSM-7600F). Prior to the analysis, the samples were coated with a thin layer of carbon.

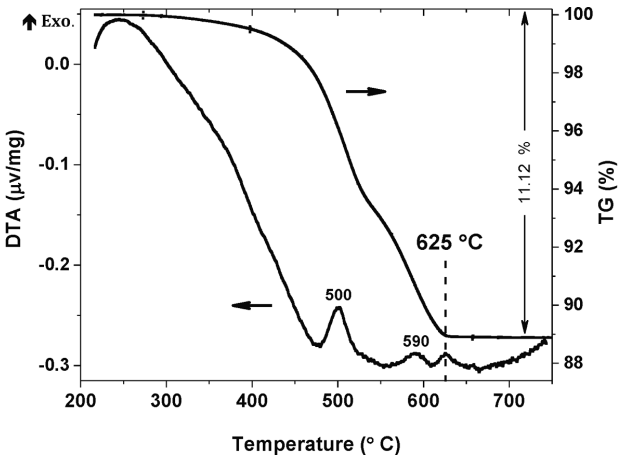

Figure 1: DTA/TG thermal analyses curves of the homogenized mixture of KNN precursors (the HOM powder)

Slika 1: Krivulji termične analize DTA/TG homogenizirane zmesi prekurzorjev KNN (prah HOM)

3 RESULTS AND DISCUSSION

3.1 Synthesis of the KNN powder at a low calcination temperature

The DTA/TG thermal analyses of the HOM powder are shown in **Figure 1**. There is a pronounced exothermic peak around 500 °C, which is accompanied by a sharp weight loss in this temperature region, which is related to the decomposition of the alkali carbonates and also to the formation of the $(K,Na)_2Nb_4O_{11}$ intermediate phase and the KNN perovskite phase from the precursors. However, there are still two minor exothermic peaks at 590 °C and 625 °C, which can be attributed to the completion of the synthesis and the final formation of KNN.[18,19] According to the TG curve, the amount of weight loss is almost zero above 625 °C. In addition, this temperature coincides with the last exothermic DTA peak.

To further explore the possible low calcination temperature, optical dilatometry of the HOM powder was performed, which is shown in **Figure 2**. The expansion started from 390 °C and it underwent a large expansion of ≈ 26 % by heating the powder compact further from 495 °C to 625 °C. Again, the temperature of 625 °C became an important temperature since the dimensional change of the sample reached a plateau at 625 °C. The dimension of the powder compact stayed constant up to 910 °C and underwent a shrinkage of ≈ 3 % during heating to 940 °C.

According to the thermal analyses of the HOM powder and the dimensional changes of the HOM powder compact, 625 °C was chosen as a possible temperature for the calcination of the KNN precursors at low temperature. The HOM powder was calcined two times for 4 h with a heating rate of 5 °C/min at 625 °C with an intermediate and final milling step similar to the homogenization process.

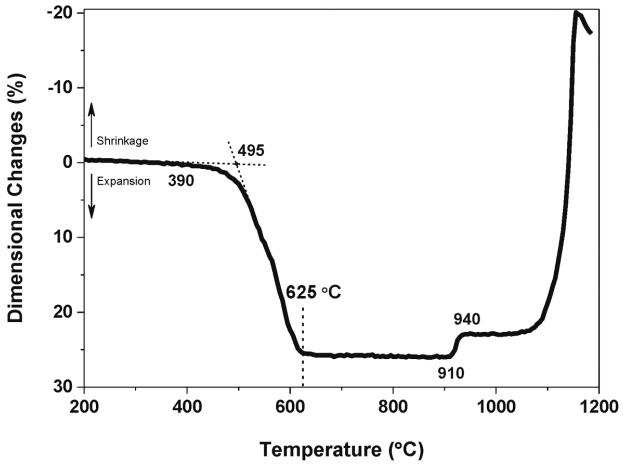

Figure 2: Dimensional changes of the powder compact of the homogenized mixture of the KNN precursors (the HOM powder)

Slika 2: Spremembe dimenzij stisnjene tabletke iz homogenizirane zmesi prekurzorjev KNN (prah HOM)

XRD patterns of the KNN calcined powders after the first and second calcinations at 625 °C are shown in **Figure 3**. For comparison, the patterns of the HOM powder that was calcined for 4 h at 800 °C and the HOM powder that was held for only 30 min at the sintering temperature of KNN, i.e., 1115 °C, are also shown in **Figure 3**. It is clear that all the peaks in these patterns can be indexed as the KNN perovskite phase and, based on the detection limit of the XRD technique, there is no trace of secondary phases or unreacted precursors in the patterns of the first and second calcined KNN powders at 625 °C. By increasing the calcination temperatures, the peaks sharpened and split, which are indications of the more homogenous structures and the growth of the crystallites.

The densification behavior of the double-calcined KNN powder at 625 °C and subsequently milled is shown in **Figure 4**. There is no change in the dimensions of the powder compact until 895 °C, but similar to the HOM powder, it again underwent a small shrinkage of ≈ 2 % during heating from 895 °C to 925 °C. We tried to decode the reason for such behavior at this temperature region and it is also a topic of another of our papers that will be published soon. However, the powder compact underwent a large shrinkage due to the sintering process, which started from ≈ 1090 °C and finally, it melted at 1150 °C. This narrow sintering window is typical for KNN-based ceramics and it is not related to the calcination temperature of the KNN.[20,21] In the inset of **Figure 4**, the particle size distribution of the double-calcined KNN powder at 625 °C and subsequently milled is shown. The d_{10}, d_{50} and d_{90} of this powder are 0.19 μm, 0.41 μm and 0.82 μm, respectively, and the powder has a unimodal distribution. The specific surface area of this powder was 18.0 m^2/g.

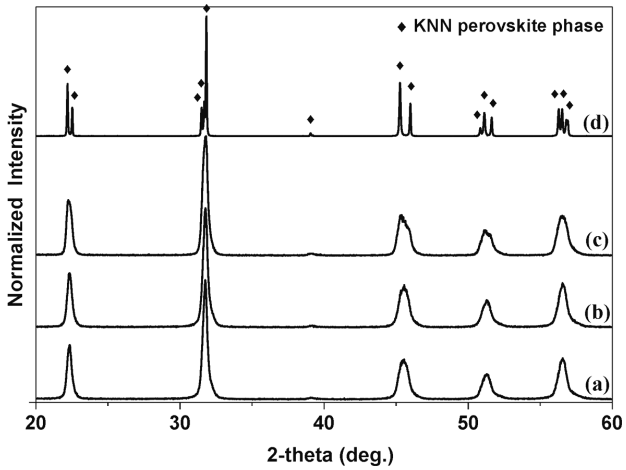

Figure 3: XRD patterns of KNN powder after: a) first calcination for 4 h at 625 °C, b) double calcination for 4 h at 625 °C, c) first calcination for 4 h at 800 °C, d) holding for 30 min at the sintering temperature of KNN (1115 °C)

Slika 3: Rentgenogram prahov KNN po: a) prvi kalcinaciji 4 h pri 625 °C, b) dvakratni kalcinaciji 4 h pri 625 °C, c) prvi kalcinaciji 4 h pri 800 °C in d) segrevanju 30 min pri temperaturi sintranja KNN (1115 °C)

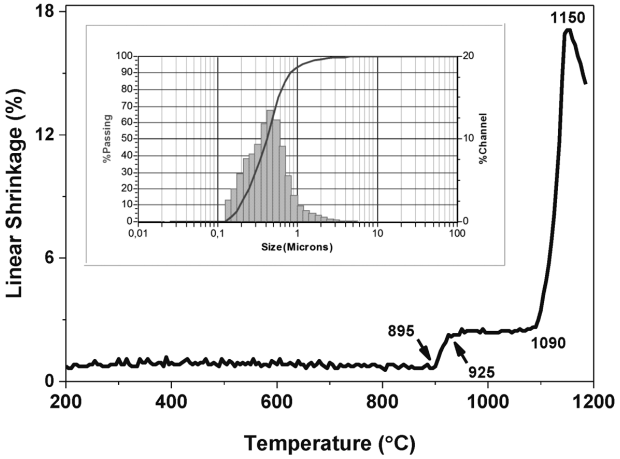

Figure 4: Densification behavior of double-calcined KNN powder for 4 h at 625 °C and subsequently milled recorded by optical dilatometry. Inset shows the particle size distribution of this powder.

Slika 4: Potek zgoščevanja dvakrat kalciniranega in mletega prahu KNN 4 h pri 625 °C, dobljen z uporabo optične dilatometrije. Vstavljena slika prikazuje porazdelitev velikosti delcev tega prahu.

The morphology, crystallite size, crystal structure and elemental composition of the double calcined KNN powder at 625 °C and subsequently milled is shown in **Figure 5**. The lower-magnification TEM BF image revealed that the calcined powder was agglomerated (**Figure 5a**). The powder was composed of agglomerates of around 500–700 nm or smaller, and of individual particles as small as 20 nm or larger (**Figure 5c**). A Selected-Area Electron Diffraction (SAED) pattern, taken from the dashed-line circled area and included as the inset in **Figure 5a**, shows a characteristic diffraction of a ring pattern with relatively continuous rings, which means the crystallites are small, in the nm range, and in a random orientation. The SAED pattern contains some brighter and more distinct spots in the rings, which indicates the presence of some larger crystallites. The electron-diffraction spots can be described by a perovskite phase with indices as shown in the inset image of **Figure 5a**.

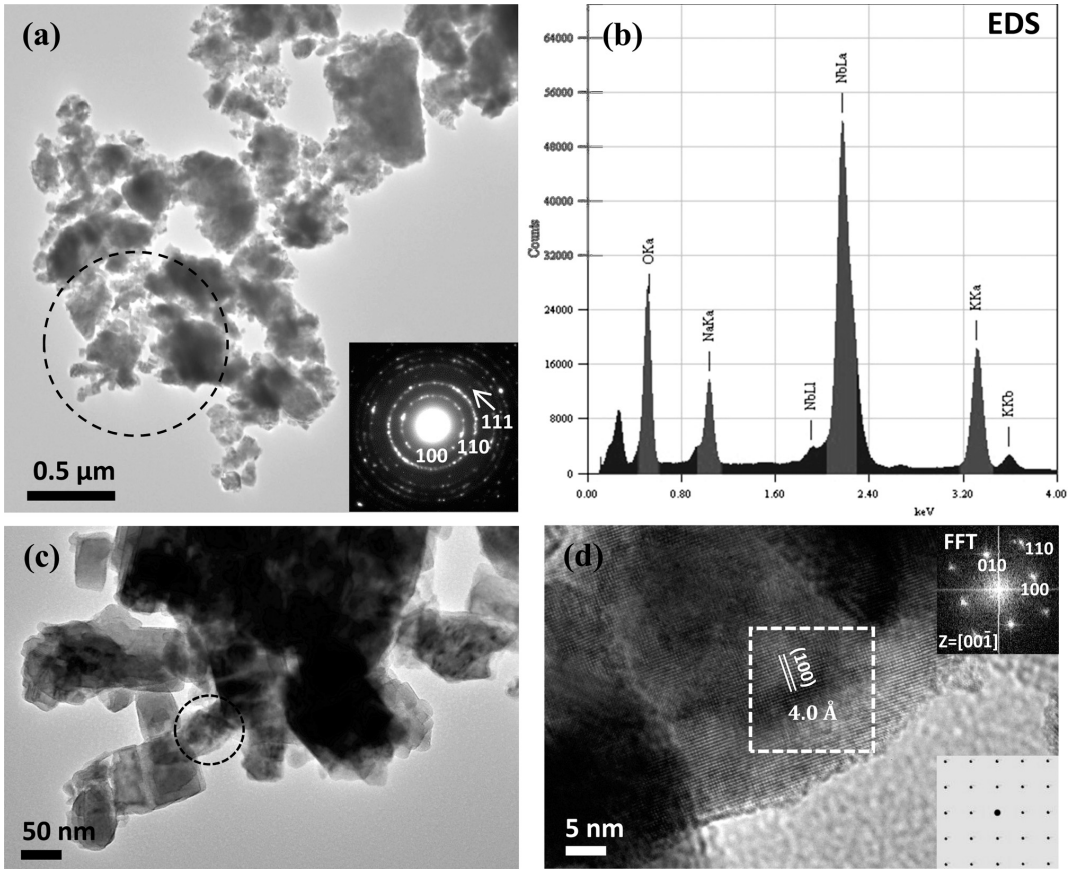

Figure 5: a) Lower magnification TEM BF image of the morphology and crystallite size of the double-calcined KNN powder at 625 °C and subsequently milled with the SAED pattern of the selected dashed-line circled area included as the inset, and b) typical EDS spectrum from the same selected dashed-line circled area in **Figure a**. c) Higher magnification TEM BF and d) HR-TEM images of this powder. From the selected dashed-line circled area of the TEM BF image, the HR-TEM image was taken. From the dashed-line circled area in the HR-TEM image, the 2D FFT and simulation image were calculated and included as the insets.

Slika 5: a) Posnetek TEM v svetlem polju (BF) pri nizki povečavi prikazuje morfologijo in velikost kristalitov dvakrat kalciniranega in mletega prahu KNN pri 625 °C z vključeno sliko uklonskega posnetka (SAED) iz izbranega obkroženega področja in b) značilno kemijsko analizo z rentgensko spektroskopijo (EDS) iz istega izbranega obkroženega področja na **sliki a**; c) posnetek TEM BF in d) visokoločljivostna slika (HR-TEM) pri višji povečavi istega prahu. Iz označenega črtkano krožnega mesta na sliki TEM BF je bil narejen posnetek HR-TEM. Iz izbranega črtkano kvadratnega področja na sliki HR-TEM sta bili izračunani vstavljeni sliki 2D hitre Fourierjeve transformacije (FFT) in simulacija.

The elemental composition was determined with EDS. A typical EDS spectrum of a selected analysis of KNN powder from the dashed-line circled area in **Figure 5a** is shown in **Figure 5b**. The analyses confirmed the presence of Nb, Na, K and O in ratios close to the KNN stoichiometry. An observation at higher magnification (**Figure 5c**) revealed particles with cuboidal shapes, which is typical for KNN powders.

The HR-TEM image with a 2D Fast Fourier Transform (FFT) inset (**Figure 5d**) shows a small KNN particle at an atomic resolution in the [00-1] zone axis. The simulated image in the inset of **Figure 5d** shows the position of the atoms in the [00-1] zone axis and corresponds to the FFT image calculated from the experimental HR-TEM image. The measured distance between the atoms from the HR-TEM image in the (100) direction is 0.40 nm, which is in very good agreement with the cell parameters of the KNN.[22]

STEM/EDS elemental mapping of the double-calcined KNN powder at 625 °C and subsequently milled is shown in **Figure 6**, with a distribution of the important comparable elements of Nb, Na and K and their overlay. The analysis nicely showed a homogeneous distribution of all three elements in the range of the detection limit of the EDS. As shown in the EDS spectrum, in some areas a small amount of Si was also detected. However, this

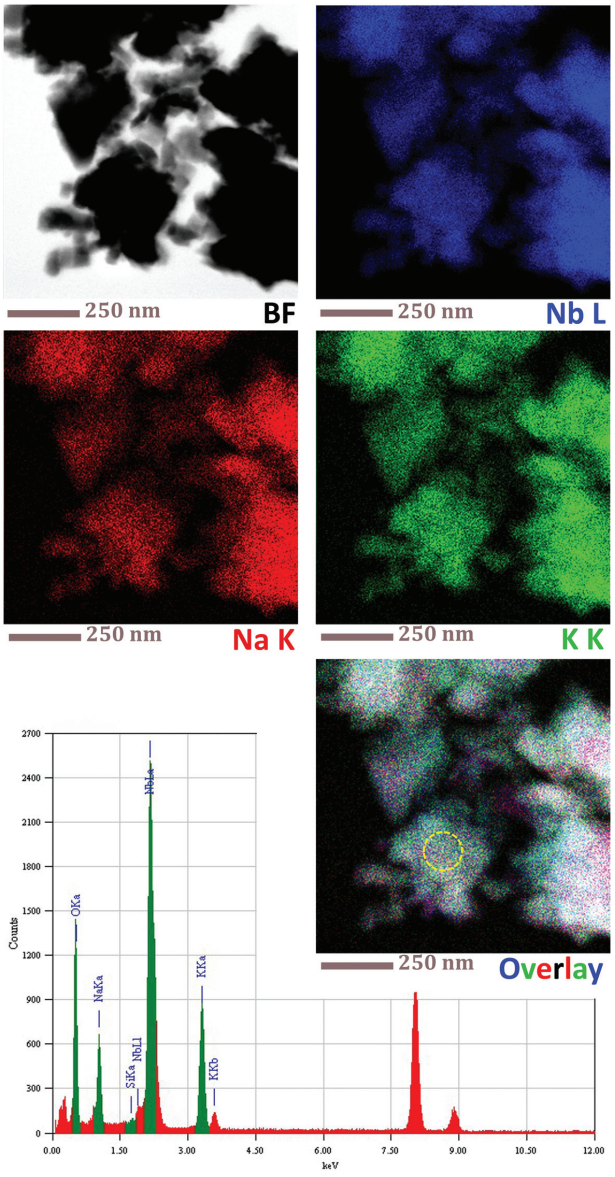

Figure 6: STEM/EDS elemental mapping of the double-calcined KNN powder at 625 °C and subsequently milled with EDS spectrum of the selected dashed-line circled area shown in the overly STEM image. Unmarked peaks at 8.04 keV and 8.90 keV belong to the Cu-$K\alpha_1$ and $K\beta_1$ characteristic X-rays, respectively, which came from the Cu TEM grid that was used as a sample holder.

Slika 6: Površinska kemijska analiza z rentgensko spektroskopijo (STEM/EDS) dvakrat kalciniranega in mletega prahu KNN pri 625 °C s spektrom EDS iz izbranega obkroženega področja, prikazanega na prekrivni sliki STEM. Neoznačeni vrhovi pri 8,04 keV in 8,90 keV pripadajo Cu-$K\alpha_1$ in $K\beta_1$ karakterističnim rentgenskim žarkom, ki izvirajo iz Cu-mrežice TEM, in ki je bila uporabljena kot nosilec vzorca.

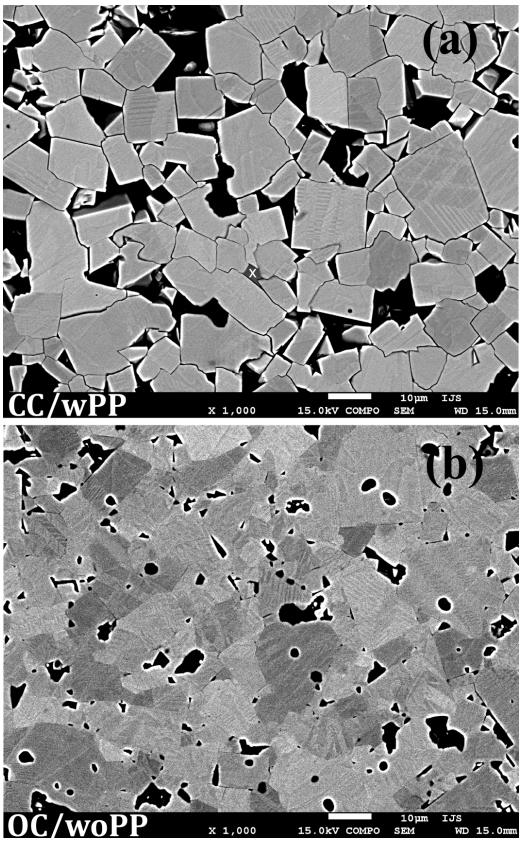

Figure 7: Orientation-contrast SEM images of a polished surface of KNN ceramics sintered under two different configurations: a) closed crucible with KNN packing powder – CC/wPP and b) open crucible without KNN packing powder – OC/woPP. The × sign in **Figure a** marks a Si-containing grain with a stoichiometry close to $K_6Nb_6Si_4O_{26}$.

Slika 7: Posnetki SEM v načinu orientacijskega kontrasta poliranih površin keramike KNN, sintrane pri dveh različnih konfiguracijah: a) zaprt lonček z zasipom KNN – CC/wPP in b) odprt lonček brez zasipa KNN – OC/woPP. Znak × na **sliki a** označuje zrno, ki vsebuje Si, katerega sestava je blizu $K_6Nb_6Si_4O_{26}$.

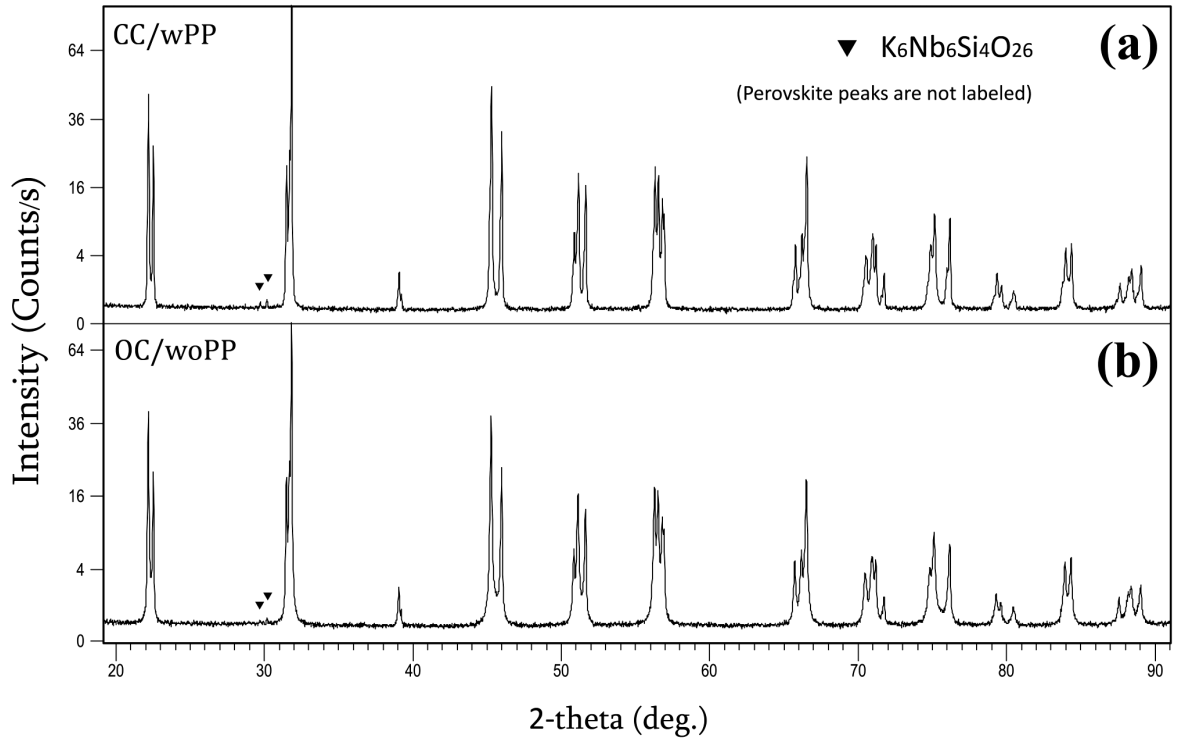

Figure 8: XRD patterns of ceramics sintered under two different configurations: a) closed crucible with KNN packing powder – CC/wPP and b) open crucible without KNN packing powder – OC/woPP

Slika 8: Rentgenogram keramike KNN, sintrane pri dveh različnih konfiguracijah: a) zaprt lonček z zasipom KNN – CC/wPP in b) odprt lonček brez zasipa KNN – OC/woPP

amount is very low for the exact characterization and its determination.

3.2 Sintering of the 625 °C-calcined KNN powder

The relative density of the ceramics sintered under the CC/wPP and OC/woPP configurations were 91.5 % and 93.4 %, respectively. **Figure 7** shows the orientation-contrast SEM images of the polished surface of the KNN ceramics sintered under the two different configurations mentioned above. The percentages of porosity, which are visible as black areas in the images, were evaluated using ImageTool version 3.00 software and measured approximately as 17.5 % and 6.5 % for the samples sintered under CC/wPP and OC/woPP configurations, respectively. Some grains may have been pulled out, which typically happens during the grinding and polishing of KNN-based ceramics. Therefore, these values are not necessarily representative of the amount of porosity in the bulk ceramics. Apart from the percentages of the porosity, the shapes of the grains are also different in these two microstructures. The CC/wPP configuration mainly resulted in cuboidal grains with plane grain boundaries, whereas the OC/woPP configuration led to almost non-polyhedral grain shapes with intragranular porosities. According to Acker et al.[23] more faceted grains can be achieved for the KNN with the amount fraction 2 % excess on the A-site. Later on, they explained that for stoichiometric KNN the excess alkali elements from the packing powder atmosphere drives the ceramic composition towards the A-site excess regime and consequently away from the ideal stoichiometric conditions for sintering dense materials.[24] This may explain why using packing powder for the suppression of the evaporation of alkali elements during sintering may cause the density of the ceramic to be even lower than the density of the unprotected sample.[25] This contradicts the popular belief about the sintering of KNN-based ceramics and raises an interesting question on the use of KNN packing powder, to what extent the addition of an alkali-rich atmosphere during sintering is beneficial for the properties of KNN-based ceramics? In addition, based on our observations, the weight losses of samples during the sintering process were significantly similar for both sintering configurations.

Figure 8 shows the XRD patterns of ceramics sintered under different sintering configurations of CC/wPP and OC/woPP. Though the KNN powder was calcined only at 625 °C and, thus, has a lower crystallinity and homogeneity compared to the usual higher-calcination-temperature powders, both sintered ceramics have highly crystalline and homogenous structures. All the main peaks can be indexed as the KNN perovskite phase with a monoclinic structure.[22] However, in both patterns, a trace of a secondary phase was found at around $2\theta \approx 30$ °. These two extra visible peaks, which are not related to the KNN perovskite phase, are in a very good accordance with the main peaks of $K_6Nb_6Si_4O_{26}$ with JCPDS

card number 01-072-0558. The existence of a Si-containing phase was also proved in the compositional analyses of the sintered samples from both sintering configurations. For example, the grain which is marked with × in **Figure 7a** represents a phase with the following atomic stoichiometry for Na : K : Nb : Si : O as (0.47 : 13.34 : 15.09 : 9.11 : 62.00) %, which matches very well with the nominal atomic stoichiometry of $K_6Nb_6Si_4O_{26}$, i.e., (14.29 : 14.29 : 9.52 : 61.90) %.

4 CONCLUSIONS

For the first time, 625 °C is suggested as the possible low-calcination temperature for the solid-state synthesis of $K_{0.5}Na_{0.5}NbO_3$ from an alkali-carbonates source. A microstructural analysis of the KNN sample processed from double-calcined KNN powder at 625 °C shows that a typical microstructure of KNN, otherwise processed with higher calcination temperatures (≈ 800 °C), can be achieved. The sintering of KNN in an open-crucible setup without using packing powder contributed to a higher density. A trace of $K_6Nb_6Si_4O_{26}$ secondary phase was found in the SEM and XRD of sintered samples, but its origin requires further investigation.

Acknowledgement

The authors would like to dedicate this paper to the memory of the late Professor Marija Kosec on the third anniversary of her death, 23rd Dec.

This work was financially supported by Ministry of Science, Research and Technology of Iran with the grant No. 38-1392-063 from Materials and Energy Research Center. In addition, the support of Jožef Stefan Institute – Electronic Ceramics Department (K5) and Institute of Metals and Technology (IMT), both from Ljubljana, Slovenia, is greatly appreciated. The contributions of Mohammad Ali Bahrevar, Alireza Aghaei, Andreja Benčan Golob, Tadej Rojac, Goran Dražić, Jurij Koruza, Katarina Vojisavljević, Julian Walker, Jernej Pavlič, Jitka Hreščak, Tina Bakarič, Marko Vrabelj, Andraž Bradeško, Maja Makarovič, Jerca Praprotnik, Tina Rucigaj, Jena Cilenšek, Silvo Drnovšek, Edi Kranjc and Maja Koblar are much appreciated. Special thanks from Mahdi go to Prof. Barbara Malič, the head of K5, for her kind and generous hosting at K5 during the visiting research period of 2014, and to Assist. Prof. Matjaž Godec, the director of IMT, for his special attention to the TEM investigations and our mutual cooperation.

5 REFERENCES

[1] B. Jaffe, W. R. Cook, H. Jaffe, Piezoelectric Ceramics, Academic Press, New York 1971

[2] European Parliament, Directive 2002/95/EU of the European Parliament and of the Council of 27 January 2003 on the restriction of the use of certain hazardous substances in electrical and electronic equipment, Official Journal of the European Union, L37 (**2003**), 19–23

[3] T. Shrout, S. Zhang, Lead-free piezoelectric ceramics: Alternatives for PZT?, Journal of Electroceramics, 19 (**2007**) 1, 111–124, doi:10.1007/s10832-007-9095-5

[4] J. Rödel, W. Jo, K. T. P. Seifert, E. M. Anton, T. Granzow, D. Damjanovic, Perspective on the development of lead-free piezoceramics, Journal of the American Ceramic Society, 92 (**2009**) 6, 1153–1177, doi:10.1111/j.1551-2916.2009.03061.x

[5] D. Damjanovic, N. Klein, J. Li, V. Porokhonskyy, What can be expected from lead-free piezoelectric materials?, Functional Materials Letters, 3 (**2010**) 1, 5–13, doi:10.1142/S1793604710000919

[6] Y. Saito, H. Takao, T. Tani, T. Nonoyama, K. Takatori, T. Homma, T. Nagaya, M. Nakamura, Lead-free piezoceramics, Nature, 432 (**2004**) 7013, 84–87, doi:10.1038/nature03028

[7] D. Jenko, A. Benčan, B. Malič, J. Holc, M. Kosec, Electron microscopy studies of potassium sodium niobate ceramics, Microscopy and Microanalysis, 11 (**2005**) 6, 572–580, doi:10.1017/S1431927605050683

[8] R. Zuo, J. Rödel, R. Chen, L. Li, Sintering and electrical properties of lead-free $Na_{0.5}K_{0.5}NbO_3$ piezoelectric ceramics, Journal of the American Ceramic Society, 89 (**2006**) 6, 2010–2015, doi:10.1111/j.1551-2916.2006.00991.x

[9] B. Malič, A. Benčan, T. Rojac, M. Kosec, Lead-free piezoelectrics based on alkaline niobates: Synthesis, sintering and microstructure, Acta Chimica Slovenica, 55 (**2008**) 4, 719–726

[10] K. Shinichiro, K. Masahiko, H. Yukio, T. Hiroshi, (K,Na)NbO_3-based multilayer piezoelectric ceramics with nickel inner electrodes, Applied Physics Express, 2 (**2009**) 11, 111401, doi:10.1143/APEX.2.111401

[11] M. Kosec, B. Malič, A. Benčan, T. Rojac, J. Tellier, Alkaline niobate-based piezoceramics: Crystal structure, synthesis, sintering and microstructure, Functional Materials Letters, 3 (**2010**) 1, 15–18, doi:10.1142/S1793604710000865

[12] J. F. Li, K. Wang, F. Y. Zhu, L. Q. Cheng, F. Z. Yao, (K, Na)NbO_3-based lead-free piezoceramics: Fundamental aspects, processing technologies, and remaining challenges, Journal of the American Ceramic Society, 96 (**2013**) 12, 3677–3696, doi:10.1111/jace.12715

[13] J. Rödel, K. G. Webber, R. Dittmer, W. Jo, M. Kimura, D. Damjanovic, Transferring lead-free piezoelectric ceramics into application, Journal of the European Ceramic Society, 35 (**2015**) 6, 1659–1681, doi:10.1016/j.jeurceramsoc.2014.12.013

[14] J. Wu, D. Xiao, J. Zhu, Potassium–sodium niobate lead-free piezoelectric materials: Past, present, and future of phase boundaries, Chemical Reviews, 115 (**2015**) 7, 2559–2595, doi:10.1021/cr5006809

[15] A. B. Haugen, F. Madaro, L. P. Bjørkeng, T. Grande, M. A. Einarsrud, Sintering of sub-micron $K_{0.5}Na_{0.5}NbO_3$ powders fabricated by spray pyrolysis, Journal of the European Ceramic Society, 35 (**2015**) 5, 1449–1457, doi:10.1016/j.jeurceramsoc.2014.11.011

[16] A. Popovic, L. Bencze, J. Koruza, B. Malič, Vapour pressure and mixing thermodynamic properties of the $KNbO_3$-$NaNbO_3$ system, RSC Advances, 5 (**2015**) 93, 76249–76256, doi:10.1039/C5RA11874C

[17] X. Vendrell, J. E. García, X. Bril, D. A. Ochoa, L. Mestres, G. Dezanneau, Improving the functional properties of $(K_{0.5}Na_{0.5})NbO_3$ piezoceramics by acceptor doping, Journal of the European Ceramic Society, 35 (**2015**) 1, 125–130, doi:10.1016/j.jeurceramsoc.2014.08.033

[18] B. Malič, A. Kupec, M. Kosec, Thermal Analysis, In: T. Schneller, R. Waser, M. Kosec, D. Payne (Eds.), Chemical Solution Deposition of Functional Oxide Thin Films, Springer, Vienna 2013, 163–179, doi:10.1007/978-3-211-99311-8_7

[19] B. Malič, D. Jenko, J. Holc, M. Hrovat, M. Kosec, Synthesis of sodium potassium niobate: A diffusion couples study, Journal of the American Ceramic Society, 91 (**2008**) 6, 1916–1922, doi:10.1111/j.1551-2916.2008.02376.x

[20] M. Kosec, D. Kolar, On activated sintering and electrical properties of $NaKNbO_3$, Materials Research Bulletin, 10 (**1975**) 5, 335–339, doi:10.1016/0025-5408(75)90002-1

[21] J. Hreščak, A. Benčan, T. Rojac, B. Malič, The influence of different niobium pentoxide precursors on the solid-state synthesis of potassium sodium niobate, Journal of the European Ceramic Society, 33 (**2013**) 15–16, 3065–3075, doi:10.1016/j.jeurceramsoc.2013.07.006

[22] J. Tellier, B. Malič, B. Dkhil, D. Jenko, J. Cilenšek, M. Kosec, Crystal structure and phase transitions of sodium potassium niobate perovskites, Solid State Sciences, 11 (**2009**) 2, 320–324, doi:10.1016/j.solidstatesciences.2008.07.011

[23] J. Acker, H. Kungl, M. J. Hoffmann, Influence of alkaline and niobium excess on sintering and microstructure of sodium-potassium niobate $(K_{0.5}\ Na_{0.5})NbO_3$, Journal of the American Ceramic Society, 93 (**2010**) 5, 1270–1281, doi:10.1111/j.1551-2916.2010.03578.x

[24] J. Acker, H. Kungl, R. Schierholz, S. Wagner, R. A. Eichel, M. J. Hoffmann, Microstructure of sodium-potassium niobate ceramics sintered under high alkaline vapor pressure atmosphere, Journal of the European Ceramic Society, 34 (**2014**) 16, 4213–4221, doi:10.1016/j.jeurceramsoc.2014.06.021

[25] P. Bomlai, P. Wichianrat, S. Muensit, S. J. Milne, Effect of calcination conditions and excess alkali carbonate on the phase formation and particle morphology of $Na_{0.5}K_{0.5}NbO_3$ powders, Journal of the American Ceramic Society, 90 (**2007**) 5, 1650–1655, doi:10.1111/j.1551-2916.2007.01629.x